Supporting information for

Consecutive Surfactant-templating Opens up New Possibilities for Hierarchical Zeolites

Erika De Oliveira Jardim[†,‡], Elena Serrano[†,‡], Juan Carlos Martínez[§], Noemi Linares[,†], and Javier García-Martínez[*,†]*

[†] Laboratorio de Nanotecnología Molecular, Departamento de Química Inorgánica, Universidad de Alicante, Ctra. San Vicente-Alicante s/n, E-03690 Alicante, Spain. www.nanomol.es

[§] ALBA Light Source, 08290 Cerdanyola del Vallés, Barcelona, Spain

[‡] These authors contributed equally

Contents

1. Experimental Procedures

1.1 Materials

USY zeolite (CBV 720, with molar ratio Si/Al = 15, as indicated by the supplier), was provided by Zeolyst®. Sodium hydroxide (98%) was supplied by Fluka. Alkyltrimethylammonium surfactants (C*n*TAB, where *n* indicates the number of carbons in the hydrophobic tail, 98%) were purchased from Sigma-Aldrich. All reagents were used without further purification. Cetyltriethylammonium (CTEAB) and cetyltripropylammonium (CTPAB) bromides were prepared by reaction of 1-bromoalkane with the appropriate trialkylamine using the method described elsewhere.[1,2] The double chain cationic surfactant dimethyldihexadecylammonium bromide, C2x16AB, was also freshly synthesized in our laboratory according to the procedure described in ref [3]. ^{1}H NMR spectra of as-synthesized surfactants were recorded with a Bruker Avance DRX500 by using $CDCl_3$ as solvent and TMS as the internal standard. Structures of surfactant molecules used in this study are given in **Scheme 2** of the main paper.

CTEAB surfactant. ^{1}H NMR (500 MHz, $CDCl_3$, 25 ºC, TMS): δ = 0.87 (3H, t), 1.21–1.47 (35H, m), 1.68–1.75 (2H, m), 3.24 –3.28 (2H, m), 3.51 (6H, q).

CTPAB surfactant. ^{1}H NMR (500 MHz, $CDCl_3$, 25 ºC, TMS): δ = 0.84 (3H, t), 1.04 (9H, t), 1.21–1.49 (26H, m), 1.63–1.84 (8H, m), 3.31–3.46 (8H, m).

C2x16AB surfactant. ^{11}H NMR (500 MHz, $CDCl_3$, 25 ºC, TMS). δ = 0.90 (6H, m), 1.13–1.50 (52 H, m), 1.72 (4H, m), 3.43 (6H, s), 3.53 (4H, m).

1.2 Synthesis of (multiple) surfactant-templated zeolites

Surfactant-templated zeolites were prepared following our previously reported procedure,[2,4–6] as described in the main paper. Samples were named using the following nomenclature: ST-*Surf* where *ST* stands for one surfactant-templating process (i.e. starting from the USY zeolite) and *Surf* is the cationic surfactant used in the synthesis.

Doble- (DST) and triple- (TST) surfactant-templated zeolites were prepared following the same procedure as described for the ST-*Surf* materials. In a typical synthesis, the mesoporous zeolite was stirred for 20 min in a new basic surfactant solution (the concentration of the surfactant and the base were kept constant for the consecutive treatments), before carrying out the hydrothermal treatment at 80 ºC, and the subsequent washing and calcination of the samples. In the case of DST samples, the starting material was the calcined surfactant-templated zeolite prepared using C16TAB, sample ST-C16TAB. Samples with two and three hydrothermal treatments were labeled as DST-*Surf* and TST-*Surf*, where *Surf* is the cationic surfactant used in the second and third treatment, respectively.

The effect of the tail length was studied by using alkyltrimethylammonium surfactants, C*n*TAB, with *n* = 12, 16 and 22. The effect of the bulkiness of the head group of the cationic surfactant in zeolite surfactant-templating was evaluated using the synthesized CTEAB and CTPAB surfactants, of larger headgroups (*i.e.* alkyl = C_2 and C_3) than C16TAB. Finally, the behavior of surfactants with more than one hydrophobic tail was analyzed by using the surfactant C2x16AB.

1.3 Materials characterization

The morphology of the resulting mesoporous zeolites was studied by transmission electron microscopy (TEM) using a JEOL JEM-1400 Plus instrument. Zeolites were grounded, suspended in ethanol and sonicated for 15 min. A few drops of this suspension were placed on a Lacey Formvar/Carbon copper grid. The ethanol was evaporated at room temperature. Further TEM analysis of the zeolites cross sections were conducted by embedding the samples in a Spurr resin and cut into slices 80 nm thin using an ultra-microtome RMC, MTXL model. The digital analysis of the TEM micrographs was done using DigitalMicrographTM 3.6.1 by Gatan. The porous texture of the materials was characterized by N_2 and Ar

adsorption at 77 K. Measurements were carried out in two devices, an AUTOSORB-6 and a Quadrasorb-Kr/MP, both from Quantachrome Instruments. The samples were previously degassed for 8 h at 250 ºC at $5{\cdot}10^{-5}$ bars. Specific surface areas were calculated using the BET method. Mesopore size and pore volume information was obtained by applying a NLDFT model.[2,4] The materials were also characterized by X-ray powder diffraction (XRD) in a SEIFERT 2002 apparatus using a CuKα (1.5418 Å) radiation. Wide angle XRD in the $2.5 < º2\theta < 50$ range was obtained using a scanning velocity of 1º min^{-1}. In order to determine the amount of surfactant incorporated into the zeolites, thermogravimetric measurements (TGA) on non-calcined zeolites were performed using a Mettler Toledo TG/SDTA analyzer under O_2:N_2 (1:4) atmosphere from room temperature to 1100 ºC at a heating rate of 10 ºC min^{-1}.

1.4 Synchrotron SAXS measurements: *in situ* and *ex situ* experiments

Small Angle X-ray Scattering (SAXS) experiments were carried out in the Non Crystalline Diffraction beamline (NCD-SWEET beamline), at ALBA synchrotron light source located in the Barcelona area, Spain (www.albasynchrotron.es). The energy of the incident photons was 12.4 KeV or equivalently a wavelength, λ, of 0.1 nm. The SAXS diffraction patterns were collected by means of a photon counting detector Pilatus3 s 1M with an active area of 168.7 x 179.4 mm^2, an effective pixel size of 172 x 172 μm^2 and a dynamic range of 20 bits. The sample-to-detector distance was set to 4062 mm, resulting in a q range with a maximum value of q = 3.6 nm^{-1}. The data reduction was treated by pyFAI[7] python code (ESRF), modified by ALBA beamline staff, that is able to do on-line azimuthal integrations from a previously calibrated file. The calibration files were created from well-known standards, i.e. Silver behenate (AgBh) and Cr_2O_3 for SAXS and WAXS respectively.

A homemade setup was designed *ad hoc* for *in situ* experiments (**Figure S1**).[5] The homemade setup consists of a capillary system connected to the reactor and to a peristaltic pump. The reactor involves a three-neck round-bottom flask equipped with a mechanical stirring device and a temperature-controlled hot plate. In the central neck, a platform with two holes, which allow the silicone tubes of the capillary connecting system to be inserted, is coupled and connected to the peristaltic pump and to a borosilicate capillary that is placed in the capillary holder. The borosilicate capillary as well as the silicon tubes diameter and length were dimensioned by taking the pumping capacity of the vacuum pump. A Teflon-like addition device, specifically designed for adding the zeolite powders, with programmed opening, is also placed in the platform coupled to the central neck, which allowed us to control the zero time. A temperature probe is also connected to the side neck of the reactor for the control of the reaction temperature. For synchrotron experiments, the capillary holder was placed on the x-y stage of the Eulerian cradle, close to the detector[5].

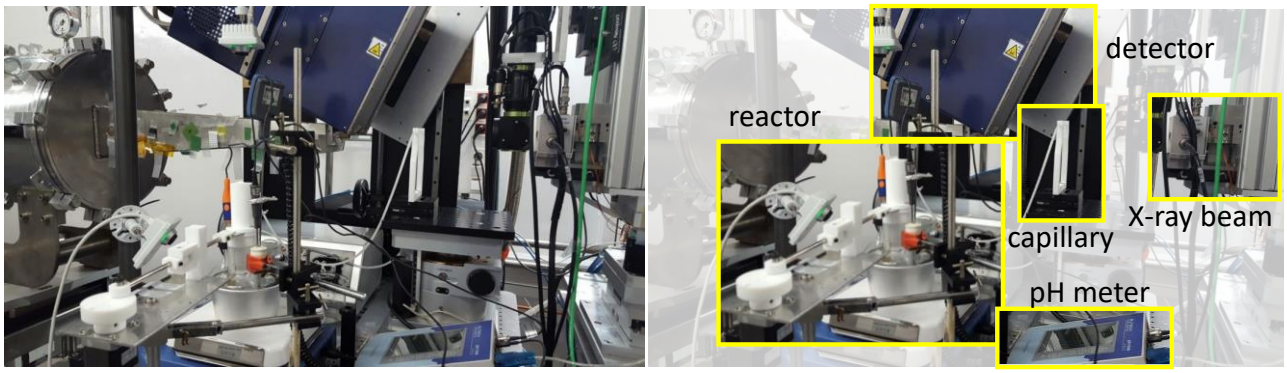

Figure S1. Optical image of the device (showing WAXS detector) and scheme of the reactor used for the *in situ* experiments in the ALBA synchrotron (beamline NCD-SWEET). Adapted from ref. [5]

2. Results and Discussion

Table S1 summarizes the textural and structural properties of the hierarchical zeolites synthesized by consecutive surfactant-templated treatments.

Table S1

Textural and structural properties of the synthesized hierarchical zeolites by ST (starting from the USY zeolite), DST (starting from the calcined ST-C16TAB zeolite) and TST (starting from the calcined DST-C22TAB), in comparison with the original USY.

Sample	V_{micro} [a] ($cm^3\ g^{-1}$)	V_{meso} [a] ($cm^3\ g^{-1}$)	D_p [a] (nm)	q [b] (nm^{-1})	d_{100} [b] (nm)	a_0 [c] (nm)	b_0 [d] (nm)	%O/T [e]
USY	0.30	0.12	–	–	–	–	–	–
ST-C16TAB	0.30	0.16	4.6	1.27	4.95	5.71	1.11	39.7
DST-C16TAB	0.26	0.23	4.4	1.27	4.95	5.71	1.31	43.8
DST-C22TAB	0.25	0.28	5.3	1.15	5.46	6.31	1.01	48.1
TST-C12TAB	0.17	0.54	4.6	1.36	4.62	5.33	0.73	59.7
ST-CTEAB	0.29	0.13	4.8	1.23	5.11	5.90	1.10	31.2
DST-CTEAB	0.28	0.21	4.5	1.23	5.11	5.90	1.40	36.3
ST-CTPAB	0.27	0.14	–	–	–	–	–	26.9
DST-CTPAB	0.28	0.17	4.6	1.24	5.07	5.85	1.25	35.0
ST-C2x16AB	0.26	0.18	–	–	–	–	–	42.6
DST-C2x16AB	0.24	0.24	5.2	n.d.*	n.d.*	n.d.*	n.d.*	45.6

[a] Volumes of micropore and mesopore and average pore size, D_p, were calculated applying the NLDFT method to the adsorption branch of the N_2 isotherms. Volume of mesopore was calculated between 2 and 8 nm. [b] d_{100} was calculated from the q value of the primary SAXS peak as $q = 2\pi/d_{100}$. [c] The lattice parameter (a_0) was calculated from the SAXS data using the formula $a_0 = 2d_{100}/\sqrt{3}$. [d] The wall thickness was determined by subtracting the average pore size (D_p) to the lattice parameter (a_0). [e] The percentage of occluded template regarding the total template (%O/T) was calculated from TGA, as the ratio between the weight loss between 120 ºC and 300 ºC and total weight loss between 120 ºC and 1000 ºC.[5] * *n.d.*: no determined.A

2.1 Mesostructured zeolites prepared by consecutive surfactant-templating treatments

2.1.1 *In situ* synchrotron SAXS studies

The evolution of the mesoporosity through multiple surfactant-templating treatments using cationic C*n*TAB surfactants with different tail length has been also *in situ* studied by synchrotron SAXS (**Figure S2**), using the experimental setup shown in **Figure S1**, which was specifically developed to *in situ* monitor the mesostructuring procedure in a synchrotron beamline.[5] Secondary surfactant templating treatments to a calcined mesoporous zeolite initially treated with C16TAB (sample ST-C16TAB) were performed using C16TAB (**Figure S2a,** DST-C16TAB sample), C22TAB (**Figure S2b,** DST-C22TAB sample) and C12TAB (**Figure S2c,** DST-C12TAB sample). ST-C16TAB sample was synthesized using low base concentration and thus, it possesses a weak peak due to the low amount of mesoporosity developed with this surfactant-templating treatment. **Figure S2** shows the time-resolved SAXS patterns of this material while performing the second hydrothermal treatment (and using the same base and surfactant concentration). The evolution of the intensity of the peak due to the mesoporosity can be easily observed in the DST-C16TAB and DST-C22TAB materials. Moreover, the larger tail of the C22TAB makes the peak shift towards lower q values, which indicates a successful modification of the mesostructured zeolite to accommodate larger pore sizes. In the case of DST-C12TAB material, the intensity of the peak does not evolve in the same way, as shorter chain surfactants tend to produce less intense and broader peaks.[8] However, there is an evident shift of the peak to higher q values with time (see the inset in **Figure S2c**), as corresponds to the shorter aliphatic chain.

The different evolutions of the intensities in the SAXS patterns for the materials depending on the surfactant used, together with the discreet shift in the mesoporous peak, make difficult the comparison of their kinetics. However, these results clearly suggest that double surfactant-templating of mesoporous zeolite with surfactants of different tails allows the modification of their mesoporous structure. These *in situ* obtained results confirm the results obtained for the solids prepared using *ex situ* conditions, which are discussed in the main paper.

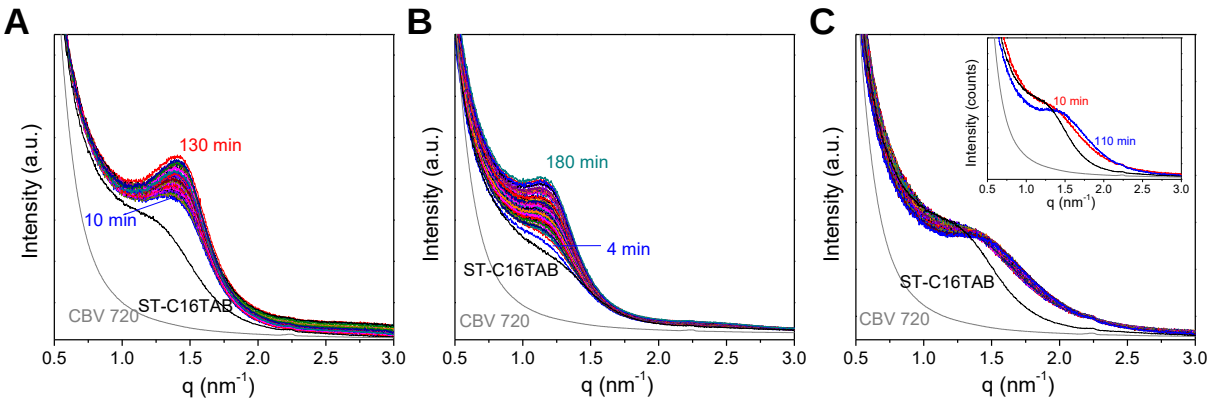

Figure S2. *In situ* time resolved synchrotron SAXS study of secondary surfactant-templating in mesoporous USY zeolite (starting material: calcined ST-C16TAB) by using as surfactants: (**A**) C16TAB (DST-C16TAB sample), (**B**) C22TAB (DST-C22TAB material) and (**C**) C12TAB (DST-C12TAB sample), in the consecutive hydrothermal treatments. Data of the parent USY zeolite (CBV 720) are shown for comparison purposes (grey).

2.1.2 Synchrotron SAXS analyses of calcined *versus* as synthesized surfactant-templated zeolites

There is a shift of the SAXS peak due to the mesoporosity to lower *q* values for the solid DST-C22TAB prepared both *in situ* (**Figure S3**) and *ex situ* (**Figure 1a** in the main paper) in comparison with the starting ST-C16TAB material. This shift is more intense in the calcined materials (*ex situ*) with regards to the *in situ* prepared materials as the starting material is a calcined solid (ST-C16TAB) while the materials *in situ* prepared by secondary hydrothermal treatments (DST) have the template still occluded. It is well known that mesoporous materials shrink through calcination and consequently the comparison between non-calcined and calcined solids masks the shift due to the higher pore-to-pore distance obtained for DST-C22TAB (**Figure S3b**).

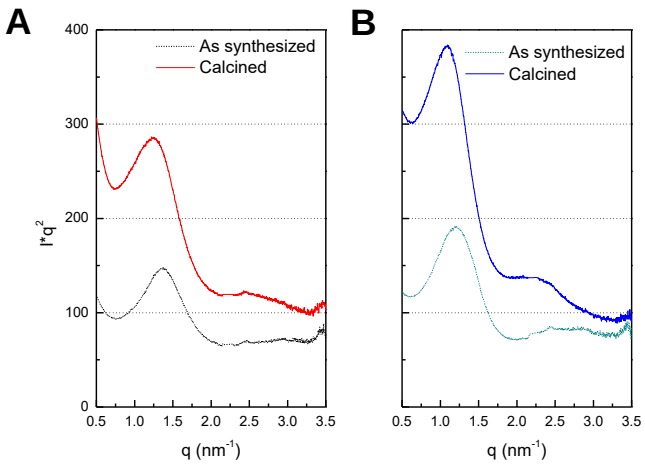

Figure S3. SAXS analyses of as-synthesized solids (solid line) in comparison with their calcined counterparts (dotted lines): (**A**) ST-C16TAB (ST of the USY using C16TAB) and (**B**) DST-C22TAB (DST of the calcined ST-C16TAB using C22TAB).

2.1.3 Control experiments performed by secondary treatments using (i) a non-micelling quaternary amine and (ii) in absence of a quaternary amine

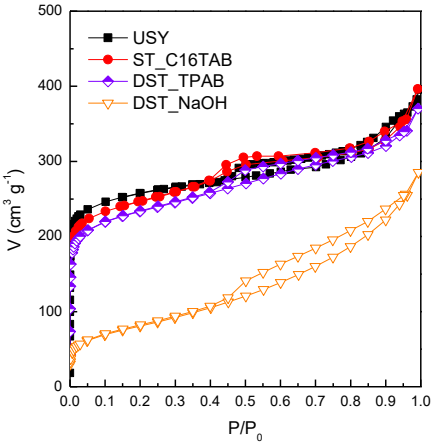

Figure S4. N_2 adsorption and desorption isotherms at 77 K of materials synthetized using (i) a non-micelling quaternary amine (DST-TPAB, purple diamonds) and (ii) in absence of a quaternary amine (DST-NaOH, orange triangles) during the secondary hydrothermal treatment using ST-C16TAB as starting material. Data of the parent USY zeolite (CBV 720, black squares) and of the ST-C16TAB (red circles) are shown for comparison purposes.

2.1.4. Consecutive surfactant-templating treatment using C12TAB and C22TAB as surfactants

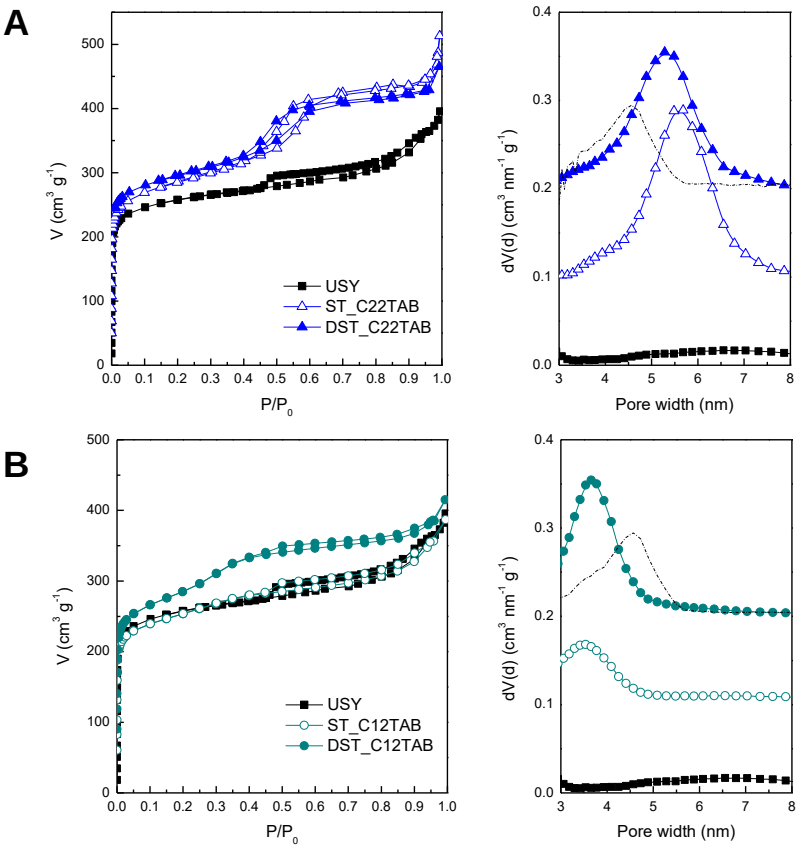

Figure S5. N_2 adsorption and desorption isotherms at 77 K, their corresponding PSD calculated by NLDFT of materials synthetized using (**A**) C22TAB and (**B**) C12TAB as surfactants by ST, ST-C22TAB (blue, empty symbols) and ST-C12TAB (cyan, empty symbols), and by DST, DST-C22TAB (blue, filled symbols) and DST-C12TAB (cyan, filled symbols). Data of the parent USY zeolite (black) are shown for comparison purposes. The curves have been shifted for the sake of clarity: N_2 isotherms +30 $cm^3\ g^{-1}$; PSD +0.1 $cm^3\ nm^{-1}\ g^{-1}$.

2.2 Relationship between the volume of mesopore and the occluded surfactant in multiple surfactant-templated zeolites

The better accessibility of the surfactants to the mesoporous zeolites can be also inferred from thermogravimetric analyses of samples before the removal of the surfactant (see **Table S1**). The calcination of CTA^+ in mesoporous materials involves three steps: (i) the elimination of the trimethylamine head group via Hofmann degradation (< 250 ºC); (ii) the oxidation of organic components (< 400 ºC), and (iii) a final oxidation process (> 400 ºC) during which carbonaceous species are removed.[9] From which, the amount of organic removed in the first step (i) is associated to the occluded template, which is responsible for the mesostructuring of the zeolite (see e.g. **Figure S6**).[5]

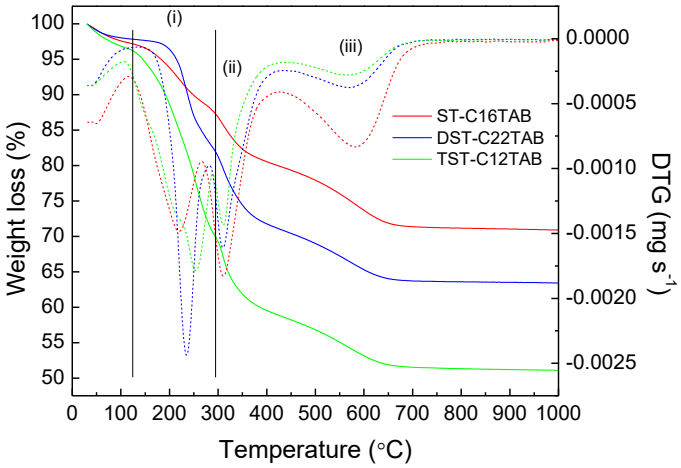

Figure S6. TG-DTG measurements of surfactant-templated USY zeolite (CBV720) with C16TAB, ST_C16TAB (red), of the calcined ST-C16TAB surfactant-templated using C22TAB, DST-C22TAB (blue), and of the calcined DST-C22TAB surfactant-templated using C12TAB, TST-C12TAB (green). Solid lines present the TGA data and in dotted lines the derivative curves of samples before the removal of the surfactant by calcination.

The ratio between the occluded, step (i) in Figure S6, and the total template present in the zeolite increases through the DST indicating that the amount of surfactant able to produce mesostructuration is higher when consecutive surfactant-templating treatments are performed. In fact, a direct linear relationship can be found between the amount of occluded template and the volume of mesoporosity generated (**Figure S7**).

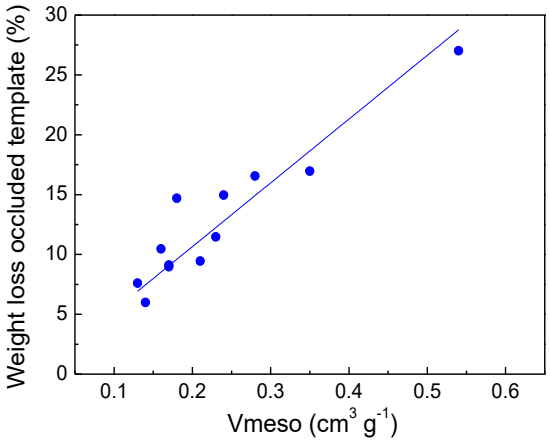

Figure S7. Weight loss due to the occluded template versus the volume of mesopore incorporated to the surfactant-templated zeolites prepared in this work.

References

(1) Buckingham, S. A.; Garvey, C. J.; Warr, G. G. Effect of Head-Group Size on Micellization and Phase Behavior in Quaternary Ammonium Surfactant Systems. *J. Phys. Chem.* **1993**, *97* (39), 10236–10244. https://doi.org/10.1021/j100141a054.

(2) Sachse, A.; Grau-Atienza, A.; Jardim, E. O.; Linares, N.; Thommes, M.; García-Martínez, J. Development of Intracrystalline Mesoporosity in Zeolites through Surfactant-Templating. *Cryst. Growth Des.* **2017**, *17* (8), 4289–4305. https://doi.org/10.1021/acs.cgd.7b00619.

(3) Engin Özdil, S.; Akbaş, H.; Boz, M. Synthesis and Physicochemical Properties of Double-Chain Cationic Surfactants. *J. Chem. Eng. Data* **2016**, *61* (1), 142–150. https://doi.org/10.1021/acs.jced.5b00367.

(4) Linares, N.; Sachse, A.; Serrano, E.; Grau-Atienza, A.; De Oliveira Jardim, E.; Silvestre-Albero, J.; Cordeiro, M. A. L.; Fauth, F.; Beobide, G.; Castillo, O.; et al. In Situ Time-Resolved Observation of the Development of Intracrystalline Mesoporosity in USY Zeolite. *Chem. Mater.* **2016**, *28* (24), 8971–8979. https://doi.org/10.1021/acs.chemmater.6b03688.

(5) Linares, N.; Jardim, E. O.; Sachse, A.; Serrano, E.; García-Martínez, J. The Energetics of Surfactant-Templating of Zeolites. *Angew. Chemie - Int. Ed.* **2018**, *57* (28), 8724–8728. https://doi.org/10.1002/anie.201803759.

(6) García-Martínez, J.; Johnson, M.; Valla, J.; Li, K.; Ying, J. Y. Mesostructured Zeolite Y—High Hydrothermal Stability and Superior FCC Catalytic Performance. *Catal. Sci. Technol.* **2012**, *2* (5), 987. https://doi.org/10.1039/c2cy00309k.

(7) Kieffer, J.; Wright, J. P. PyFAI: A Python Library for High Performance Azimuthal Integration on GPU. *Powder Diffr.* **2013**, *28* (S2), S339–S350. https://doi.org/10.1017/S0885715613000924.

(8) Kruk, M.; Jaroniec, M.; Sayari, A. Adsorption Study of Surface and Structural Properties of MCM-41 Materials of Different Pore Sizes. *J. Phys. Chem. B* **1997**, *101* (4), 583–589. https://doi.org/10.1021/jp962000k.

(9) Kleitz, F.; Schmidt, W.; Schüth, F. Evolution of Mesoporous Materials during the Calcination Process: Structural and Chemical Behavior. *Microporous Mesoporous Mater.* **2001**, *44–45*, 95–109. https://doi.org/10.1016/S1387-1811(01)00173-1.